Received: Added at production | Revised: Added at production | Accepted: Added at production

DOI: xxx/xxxx

SHORT COMMUNICATION

Addendum to the paper "High-order symmetric cubature rules for tetrahedra and pyramids"

Jan Jaśkowiec[1] | N. Sukumar*[,2]

[1]Faculty of Civil Engineering, Cracow University of Technology, Warszawska 24, 31-155 Cracow, Poland

[2]Department of Civil and Environmental Engineering, University of California, Davis, CA 95616, USA

Correspondence

*N. Sukumar, Department of Civil and Environmental Engineering, University of California, One Shields Avenue, Davis, CA 95616, USA

Email: nsukumar@ucdavis.edu

In Jaśkowiec and Sukumar (Int J Numer Methods Eng., doi: 10.1002/nme.6528, 2020), we presented high-order ($p = 2$–20) symmetric cubatures rules for tetrahedra and pyramids. This algorithm was sensitive to the initial location of the cubature nodes, and it did not converge for $p > 11$ over prisms and hexahedra (cubes). In this addendum, we resolve this issue and obtain high-order symmetric rules over prisms and cubes. For the prism, we use the initial guess for the cubature rule as the tensor product of a cubature rule over a triangle and a univariate Gauss quadrature rule, and for the cube the initial guess is the tensor product of univariate Gauss quadrature rules. Verification and convergence tests are presented to affirm the accuracy of the cubature rules. On applying the cubature algorithm described in Jaśkowiec and Sukumar (Int J Numer Methods Eng., 121 (11), 2418-2436, 2020), we also construct non-symmetric high-order ($p = 2$–20) cubature rules over prisms, cubes, and pyramids. In the Supplementary Materials, all cubature rules (128 digits of precision) are provided in a text file and in `Matlab`® format.

KEYWORDS:

symmetric and non-symmetric cubature rules; strictly interior integration points; positive weights; prismatic element; hexahedral element; pyramidal element

1 | INTRODUCTION

In a recent paper,[1] the authors presented high-order ($p = 2$–20) symmetric cubatures rules for tetrahedra and pyramids. It was noted that for $p > 11$ over prisms and hexahedra (cubes), there was nonconvergence in the cubature algorithm. We attributed this nonconvergence to the algorithm's strong dependence on the initial guess for the cubature nodes (randomly chosen or from lower-order rules). In this communication, we resolve this issue and obtain high-order symmetric cubature rules for prisms and cubes. For prisms, we use the initial guess for the cubature rule as the tensor product of a cubature rule over a triangle and a

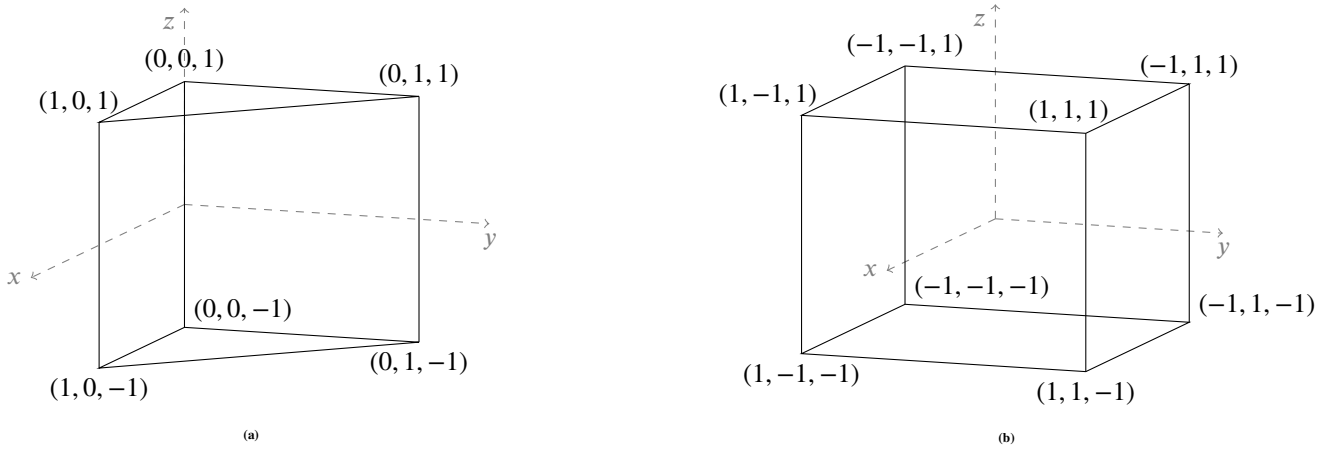

FIGURE 1 Reference elements. (a) Prism and (b) Hexahedron (biunit cube).

univariate Gauss quadrature rule, and for cubes the initial guess is the tensor product of univariate Gauss quadrature rules. In these tensor-product rules, symmetry orbits have to be identified, which are shown in Felippa,[2] Witherden and Vincent,[3] and Kubatko et al.[4] In the supplementary materials, symmetric cubature rules for prisms and cubes are made available. Additionally, as an extension of the contribution in Jaśkowiec and Sukumar,[5] non-symmetric cubature rules for the pyramid, prism and cube, are also constructed and provided in the supplementary materials. In Section 2, symmetry relations for the prism and the hexahedron (biunit cube) are presented, and symmetric cubature rules are constructed in Section 3. Verification and convergence tests to assess the accuracy of the cubature rules are presented in Section 4, and the main conclusions are summarized in Section 5.

2 | REFERENCE ELEMENTS AND SYMMETRY RELATIONS

Our objective is to obtain symmetric cubature schemes over a prism and a cube. As problem domains, we consider the reference prism R and the reference hexahedron (biunit cube) H that are shown in Fig. 1. We use monomials as basis functions over these reference domains. The integral of a monomial of order (degree) $p = r + s + t$ over R and H are:

$$\int_R x^r y^s z^t \, d\boldsymbol{x} = \begin{cases} \dfrac{2\, r!\, s!}{(t+1)(r+s+2)!} & \text{if } t \text{ is even} \\ 0 & \text{otherwise} \end{cases}, \qquad \int_H x^r y^s z^t \, d\boldsymbol{x} = \begin{cases} \dfrac{8}{(r+1)(s+1)(t+1)} & \text{if } r, s \text{ and } t \text{ are all even} \\ 0 & \text{otherwise} \end{cases}. \tag{1}$$

For symmetric arrangement of integration points over the prism (see Fig. 1a), it is convenient to use barycentric coordinates in the xy-plane.[6,3] Six possible permutation stars for the prism $\{S_i^R\}_{i=1}^6$ are presented in Table 1, where the values within the square brackets are permuted. For the hexahedron shown in Fig. 1b, any point in the element is expressed using Cartesian coordinates. For this element, the symmetry orbits $\{S_i^H\}_{i=1}^7$ are listed in Table 2.

TABLE 1 Symmetry orbits using barycentric coordinates in the xy-plane for the reference prism.

symmetry orbits	permutation stars in barycentric coordinates	$\lvert S_i^R \rvert$
S_1^R	$\left(\frac{1}{3}, \frac{1}{3}, \frac{1}{3}, 0\right)$	1
S_2^R	$\left(\frac{1}{3}, \frac{1}{3}, \frac{1}{3}, \pm c\right)$	2
S_3^R	$\big([a, a, 1-2a], 0\big)$	3
S_4^R	$\big([a, a, 1-2a], \pm c\big)$	6
S_5^R	$\big([a, b, 1-a-b], 0\big)$	6
S_6^R	$\big([a, b, 1-a-b], \pm c\big)$	12

TABLE 2 Symmetry orbits for the reference hexahedron.

symmetry orbits	permutation stars in global coordinates	$\lvert S_i^H \rvert$
S_1^H	$\big(0, 0, 0\big)$	1
S_2^H	$\big([\pm a, 0, 0]\big)$	6
S_3^H	$\big([\pm a, \pm a, \pm a]\big)$	8
S_4^H	$\big([\pm a, \pm a, 0]\big)$	12
S_5^H	$\big([\pm a, \pm b, 0]\big)$	24
S_6^H	$\big([\pm a, \pm a, \pm b]\big)$	24
S_7^H	$\big([\pm a, \pm b, \pm c]\big)$	48

3 | SYMMETRIC CUBATURE SCHEMES: PRISM AND CUBE

The cubature algorithm proposed in Jaśkowiec and Sukumar[1] is implemented to generate high-order symmetric cubature schemes over the reference prism and the reference hexahedron shown in Fig. 1. The computations are done using double-precision arithmetic and the final steps of the algorithm are performed in high-precision (160 digits) arithmetic.

For the prism and the cube, convergence of the algorithm is very sensitive to the initial guess for the cubature nodes. When the initial cubature nodes are randomly generated or chosen using combination of lower order integration schemes, the algorithm fails to converge for higher orders.[1] We resolve this herein by generating the initial nodal sets as Cartesian products. For the prism, we use the Cartesian product of symmetric cubature rules over a triangle and univariate Gauss quadrature rules. For the cube, tensor-product univariate Gauss quadrature rules are chosen as the initial set. This approach leads to initial sets with relatively large number of nodes. However, the cubature algorithm is able to significantly reduce the number of nodes in the final cubature rule. For example, if $p = 15$, the initial set over a prism consists of $49 \times 9 = 441$ nodes, while there are $9 \times 9 \times 9 = 729$ nodes for the cube. The final cubatures over the prism and cube have 238 nodes and 256 nodes, respectively.

The initial sets generated by the Cartesian products are symmetric, but the specific symmetry orbits have to be firstly identified over the reference elements to start the algorithm. For the prism, symmetry orbits are naturally taken from the combination

TABLE 3 Number of integration points and combination of symmetry orbits for various symmetric prismatic cubature rules. Our results are compared to the rules presented in Witherden and Vincent.[3]

	This work								Witherden and Vincent[3]							
p	n	$\lvert S_1^R\rvert$	$\lvert S_2^R\rvert$	$\lvert S_3^R\rvert$	$\lvert S_4^R\rvert$	$\lvert S_5^R\rvert$	$\lvert S_6^R\rvert$	r_w	n	$\lvert S_1^R\rvert$	$\lvert S_2^R\rvert$	$\lvert S_3^R\rvert$	$\lvert S_4^R\rvert$	$\lvert S_5^R\rvert$	$\lvert S_6^R\rvert$	r_w
2	5	0	1	1	0	0	0	0.755	5	0	1	1	0	0	0	0.750
3	8	0	1	2	0	0	0	0.553	8	0	1	0	0	1	0	0.407
4	11	0	1	1	1	0	0	0.458	11	0	1	1	1	0	0	0.458
5	16	1	0	1	2	0	0	0.177	16	1	0	1	2	0	0	0.231
6	28	0	2	2	1	0	1	0.151	28	0	2	2	1	0	1	0.161
7	35	0	1	1	2	1	1	0.157	35	0	1	1	2	1	1	0.157
8	46	0	2	2	4	0	1	0.136	46	0	1	1	2	1	1	0.136
9	59	0	1	1	6	1	1	0.164	60	1	1	1	6	1	1	0.063
10	84	1	1	3	6	0	3	0.092	85	0	2	3	5	1	3	0.024
11	99	0	3	1	8	1	3	0.069	–	–	–	–	–	–	–	–
12	136	0	2	2	7	2	6	0.022	–	–	–	–	–	–	–	–
13	162	0	0	0	12	3	6	0.113	–	–	–	–	–	–	–	–
14	194	0	1	2	12	3	8	0.068	–	–	–	–	–	–	–	–
15	238	0	2	4	8	1	14	0.046	–	–	–	–	–	–	–	–
16	287	0	1	3	9	3	17	0.022	–	–	–	–	–	–	–	–
17	338	0	1	0	19	1	18	0.041	–	–	–	–	–	–	–	–
18	396	0	0	0	19	1	23	0.040	–	–	–	–	–	–	–	–
19	420	0	3	4	18	3	23	0.028	–	–	–	–	–	–	–	–
20	518	0	1	2	22	3	30	0.030	–	–	–	–	–	–	–	–

of the triangle symmetry orbits in the xy-plane and location of univariate Gauss quadrature rules in the z-direction. The hexahedral symmetry orbits are directly obtained by matching the univariate quadrature nodes in the x-, y- and z-directions to the permutation stars in Table 2.

In Tables 3, symmetric prismatic cubature rules for orders $p = 2$ to $p = 20$ are presented. The number of integration points, combination of symmetry orbits, and values of the parameter $r_w = \min(w_i)/\max(w_i)$ (measures the quality of the cubature scheme) are indicated. Up to $p = 10$, numerical integration results from our integration schemes are compared to those obtained using the rules from Witherden and Vincent.[3] For $p = 2$ to $p = 8$, we obtain the same number of cubature nodes as in Witherden and Vincent,[3] and for $p = 9$, 10 we have managed to obtain cubatures with fewer number of nodes. For $p = 2$–10, the values of r_w for our cubatures and those of Witherden and Vincent[3] are close. Similar information on the cubatures over the cube is presented in Table 4. Symmetric cubature rules are provided only for odd values of p since the even orders (one less than the odd p) have the same rule. Cubature rules for odd orders over the cube have been obtained up to $p = 21$, with schemes for $p = 5$, 9 being the same as in Witherden and Vincent.[3] Our cubature rules from $p = 13$ to $p = 21$ are new. For higher order prismatic cubatures, it is observable that two types of symmetric orbits, S_4^R and S_6^R, dominate over other orbits. For higher order hexahedral cubatures, S_6^H is the dominant symmetric orbit.

TABLE 4 Number of integration points and combination of symmetry orbits for various symmetric hexahedral cubature rules. Our results are compared to the rules presented in Witherden and Vincent.[3]

	This work									Witherden and Vincent[3]								
p	n	$\lvert S_1^H\rvert$	$\lvert S_2^H\rvert$	$\lvert S_3^H\rvert$	$\lvert S_4^H\rvert$	$\lvert S_5^H\rvert$	$\lvert S_6^H\rvert$	$\lvert S_7^H\rvert$	r_w	n	$\lvert S_1^H\rvert$	$\lvert S_2^H\rvert$	$\lvert S_3^H\rvert$	$\lvert S_4^H\rvert$	$\lvert S_5^H\rvert$	$\lvert S_6^H\rvert$	$\lvert S_7^H\rvert$	r_w
3	6	0	1	0	0	0	0	0	1.0	6	0	1	0	0	0	0	0	1.0
5	14	0	1	1	0	0	0	0	0.378	14	0	1	1	0	0	0	0	0.378
7	34	0	1	2	1	0	0	0	0.246	34	0	1	2	1	0	0	0	0.336
9	58	0	1	2	1	0	1	0	0.116	58	0	1	2	1	0	1	0	0.116
11	90	0	1	3	1	0	2	0	0.055	90	0	1	3	1	0	2	0	0.105
13	154	0	1	2	1	1	4	0	0.097	–	–	–	–	–	–	–	–	–
15	256	0	2	2	1	2	5	1	0.067	–	–	–	–	–	–	–	–	–
17	346	0	1	2	3	2	6	2	0.005	–	–	–	–	–	–	–	–	–
19	454	0	1	2	0	3	11	2	0.039	–	–	–	–	–	–	–	–	–
21	580	0	2	2	0	3	12	4	0.024	–	–	–	–	–	–	–	–	–

As in Jaśkowiec and Sukumar,[1] the reader can find the listing of the cubature points and weights in the supplementary materials, where data with 128 digits of precision are provided in two forms: compact where only the unique values in the symmetry orbits (free variables) are given and extended with all points and weights given in column-format $x\ y\ z\ w$. Cubature rules are listed in a text file as well as in MATLAB® binary format.

4 | NUMERICAL TESTS

We present verification and convergence tests for the symmetric prismatic and hexahedral cubature rules using double-precision arithmetic. The aim of the verification tests is to ensure that the cubature rules deliver close to machine-precision accuracy for the integration of polynomial functions. In the convergence tests, nonpolynomial functions are considered to assess the performance of the cubature rules. For comparison purposes, the same tests are also carried out for the cubature rules of Witherden and Vincent.[3] Symmetric cubature rules for the prism are readily obtained as the Cartesian product of cubature rules over the triangle and univariate Gauss quadrature rules. Similarly, symmetric hexahedral cubature rules can be constructed using the Cartesian product of cubature rules over the square and univariate Gauss quadrature rules. Symmetric hexahedral cubature rules can also be generated using the tensor product (1D $\times$ 1D $\times$ 1D) of univariate Gauss quadrature rules. The two-dimensional cubature rules for the triangle and the square are taken from Witherden and Vincent.[3] Such cubature rules over the prism and the hexahedron require far more number of cubature nodes than the lower bound estimate for n. We also compare the accuracy and efficiency of our symmetric cubature rules with the symmetric cubature rules that are generated by these Cartesian product constructions over the prism and the hexahedron. A single verification test is presented in Section 4.1, and in the Section 4.2

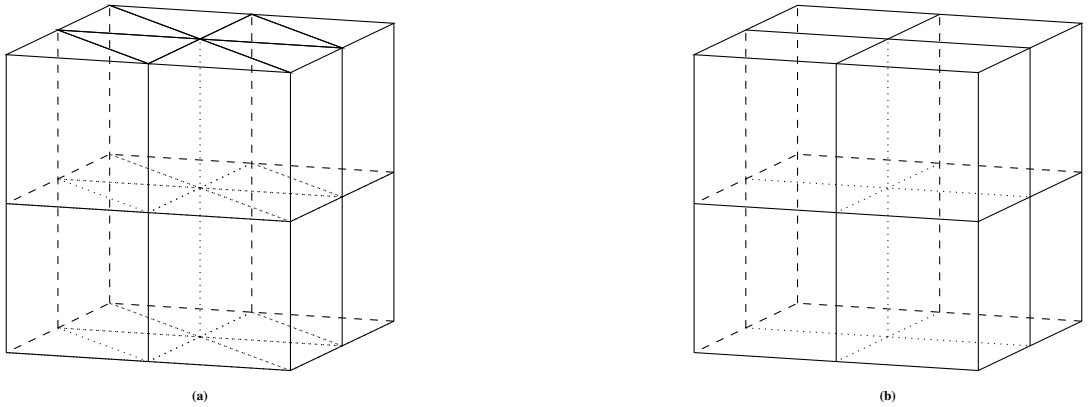

FIGURE 2 Cube meshed by (a) 16 prisms and (b) 8 hexahedra.

we consider convergence tests for an exponential function over the biunit cube $C = [-1, 1]^3$ and a trigonometric function over a semi-cylindrical domain.

For the tests, the biunit cube C is meshed with 16 prismatic elements or 8 hexahedral elements (see Fig. 2). For all tests, the relative error is defined as

$$R = \frac{|I - I_q|}{|I|},$$

where I is the exact value of the integral, and I_q is the numerically computed value of the integral using the cubature rule.

4.1 | Verification tests on the biunit cube

For each p, 100 random polynomials $f(\boldsymbol{x})$ are generated and then integrated over the biunit cube, We choose the order of $f(\boldsymbol{x})$ to be the same as the order of the cubature to be checked. The accuracy of any cubature rule of order p should be within machine-precision for any polynomial up to order p over a mesh of prismatic or hexahedral (cubes) elements that partitions C. The results of the numerical tests are presented in Table 5 for prismatic elements and in Table 6 for hexahedral elements. The maximum as well as the algebraic mean values of the relative integration errors from a set of 100 tests for each p are presented. From Table 5 and Table 6, we observe that for each p the errors oscillate about machine precision, thereby establishing the correctness of the cubature rules.

4.2 | Convergence tests

Convergence tests using exponential and trigonometric functions are conducted.[1,5] The test for the exponential function is performed over the biunit cube. The trigonometric test function is integrated over a semi-cylindrical domain (curved sides), which is generated by a nonlinear transformation from the biunit cube.[5]

TABLE 5 Integration errors for verification test over the biunit cube that is meshed with 16 prisms. Comparisons are made to results obtained using the schemes presented in Witherden and Vincent,[3] as well as the cubature rules generated by the Cartesian product of triangular cubatures and univariate Gauss quadrature rules. The listing is the maximum and mean values of the error from hundred tests for each p.

	This work			Witherden and Vincent[3]			Tensor product (2D × 1D)		
p	n	max	mean	n	max	mean	n	max	mean
		$R \times 10^{16}$			$R \times 10^{16}$			$R \times 10^{16}$	
2	5	27	3	5	28	3	6	52	4
3	8	26	3	8	23	3	12	46	4
4	11	67	5	11	56	4	18	8	5
5	16	65	5	16	91	5	21	63	7
6	28	65	6	28	30	5	48	70	6
7	35	45	5	35	50	6	60	74	8
8	46	189	10	46	91	8	80	224	12
9	59	144	10	60	117	6	95	134	9
10	84	83	7	85	207	10	150	277	11
11	99	248	10	–	–	–	168	193	15
12	136	164	11	–	–	–	231	311	23
13	162	195	17	–	–	–	259	239	20
14	194	835	20	–	–	–	336	867	29
15	238	296	22	–	–	–	392	355	19
16	287	383	13	–	–	–	495	411	15
17	338	140	13	–	–	–	540	79	13
18	396	108	13	–	–	–	670	328	17
19	420	67	9	–	–	–	730	100	13
20	518	361	17	–	–	–	869	679	30

4.2.1 | Exponential test function

We consider the exponential test function[1]

$$f(\boldsymbol{x}) = \exp(\alpha x + \beta y + \gamma z), \tag{2a}$$

whose integral over the biunit cube C is:

$$I = \int_C f(\boldsymbol{x})\, d\boldsymbol{x} = \frac{\left[\exp(\alpha) - \exp(-\alpha)\right]\left[\exp(\beta) - \exp(-\beta)\right]\left[\exp(\gamma) - \exp(-\gamma)\right]}{\alpha\beta\gamma}. \tag{2b}$$

For this test, we choose $\alpha = 5$, $\beta = 2$, and $\gamma = 1$, and the exact value of the integral is $I = 2.5302052232599806 \times 10^2$.

In Fig. 3, convergence curves of the relative integration error are shown as a function of p and n for the prismatic and hexahedral meshes. Up to order $p = 10$ and $p = 11$ for prismatic and hexahedral meshes, respectively, the relative errors for ours schemes and those of Witherden and Vincent[3] are proximal. For the mesh with prismatic elements, convergence is nonmonotonic, whereas convergence is monotonic over the mesh with hexahedral elements. For $p > 10$, the accuracy in the integration improves with our

TABLE 6 Integration errors for verification test over the biunit cube that is meshed with 8 hexahedra (cubes). Comparisons are made to results obtained using the schemes presented in Witherden and Vincent,[3] as well as cubature rules over the cube that are generated using Cartesian products (2D × 1D and 1D × 1D × 1D) of lower-dimensional integration rules. The listing is the maximum and mean values of the error from hundred tests for each p.

,

	This work			Witherden and Vincent[3]			Tensor product (2D × 1D)			Tensor product (1D × 1D × 1D)		
p	n	max	mean	n	max	mean	n	max	mean	n	max	mean
		$R \times 10^{16}$			$R \times 10^{16}$			$R \times 10^{16}$			$R \times 10^{16}$	
3	8	27	4	6	36	5	8	48	3	8	34	4
5	14	4	2	14	66	6	24	34	4	27	89	6
7	34	30	13	34	103	7	48	114	6	64	191	8
9	58	103	7	58	133	8	100	277	15	125	100	9
11	90	99	8	90	193	14	168	348	19	216	620	17
13	154	152	12	–	–	–	259	675	19	343	167	16
15	256	594	29	–	–	–	384	437	32	512	202	18
17	346	379	18	–	–	–	540	294	20	729	180	17
19	454	610	23	–	–	–	720	864	30	1000	159	16
21	580	354	23	–	–	–	935	1664	33	1331	136	16

schemes, and reaches close to $\mathcal{O}(10^{-15})$ for $p = 20$ (prism) and $p = 21$ (hexahedron). From Fig. 3, we observe that the relative errors for our schemes and those obtained using tensor-product cubature rules are of the same order of accuracy. However, for a fixed p (cubature order), our cubature rules require far fewer number of nodes (smaller n); for a fixed n, our rules deliver better accuracy (see Fig. 3b and Fig. 3d).

4.2.2 | Integration over a semi-cylindrical domain

In this example, the function $f = \sin(x^2+y^2)$ is integrated over a semi-cylindrical domain Ω of height 2, inner radius $R_1 = \sqrt{\pi/2}$ and outer radius $R_2 = \sqrt{3\pi}$. Illustration of the domain as well as the expression for the geometric map appear in Jaśkowiec and Sukumar.[5] The exact value of the integral of f over Ω is equal to π. The semi-cylindrical domain is meshed with 16 prismatic elements or 8 hexahedral elements. The relative error in the numerical integration as a function of the order p is presented in Fig. 4. Up to $p = 10$ in Fig. 4a and $p = 11$ in Fig. 4b, our schemes and those from Witherden and Vincent[3] have similar accuracy. Nonmonotonic convergence is observed for prismatic elements and monotonic convergence is realized when hexahedral elements are used. In both cases, integration error increases for the highest p, since close to machine-precision accuracy has already been attained. The tensor-product cubature rules deliver the same level of integration accuracy as our cubature rules. As in the previous example, we observe that for a fixed p, our cubature rules require far fewer number of nodes, and for a fixed n, our rules deliver better accuracy (see Fig. 4b and Fig. 4d).

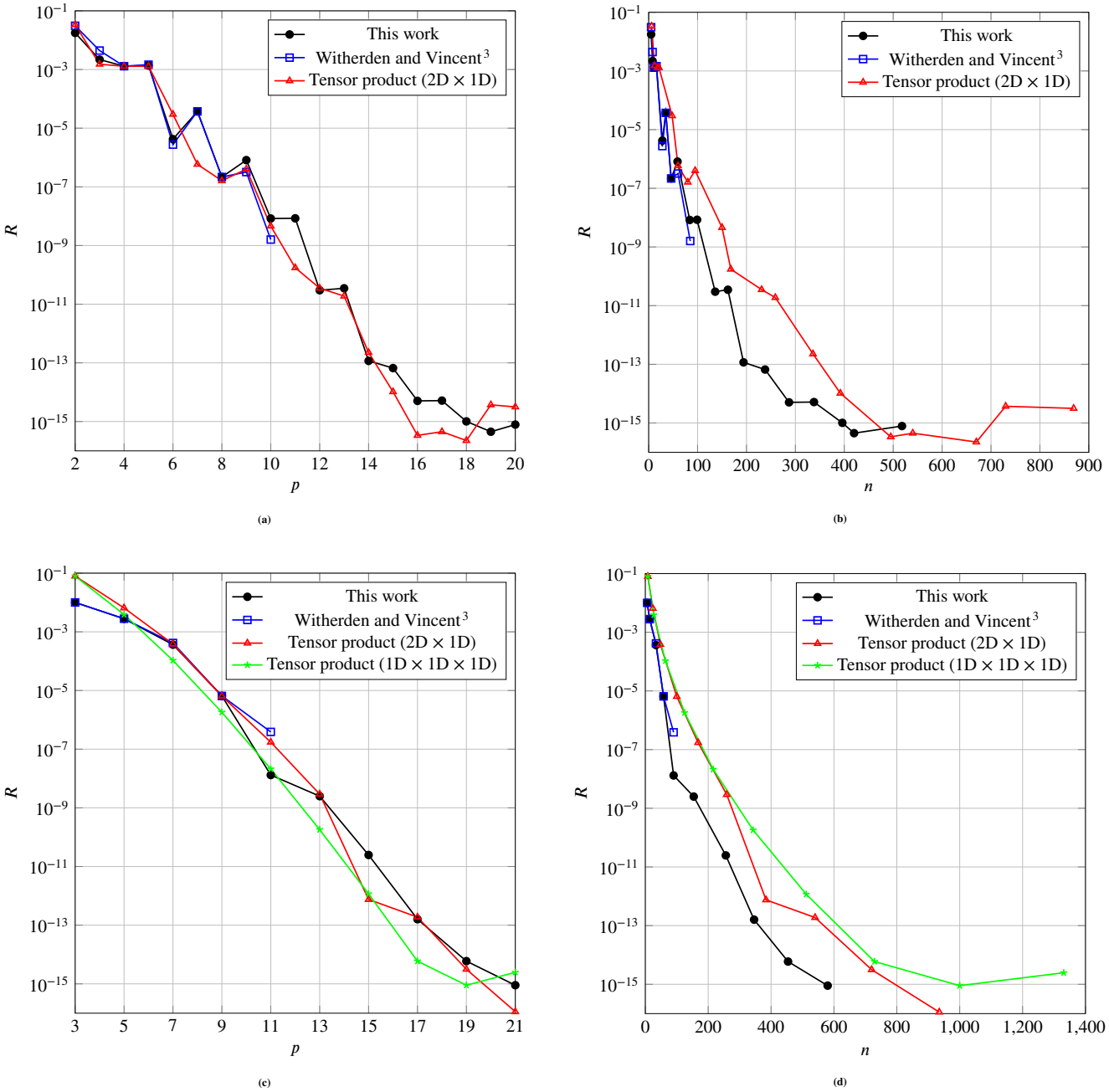

FIGURE 3 Relative error in the integration of the exponential function in (2) ($\alpha = 5$, $\beta = 2$, $\gamma = 1$) over the biunit cube, which is meshed with (a), (b) 16 prismatic elements and (c), (d) 8 hexahedral elements. Results are shown as a function of p (cubature order) and n (number of cubature nodes).

5 | CONCLUSIONS

In this addendum, we extend the contributions of Jaśkowiec and Sukumar[1] by constructing high-order symmetric cubatures for the prism and the hexahedron (biunit cube). We constructed symmetruc cubature rules up to order $p = 20$ for the prism and up to order $p = 21$ for the cube. In the literature, the highest orders that are currently available for symmetric cubatures are

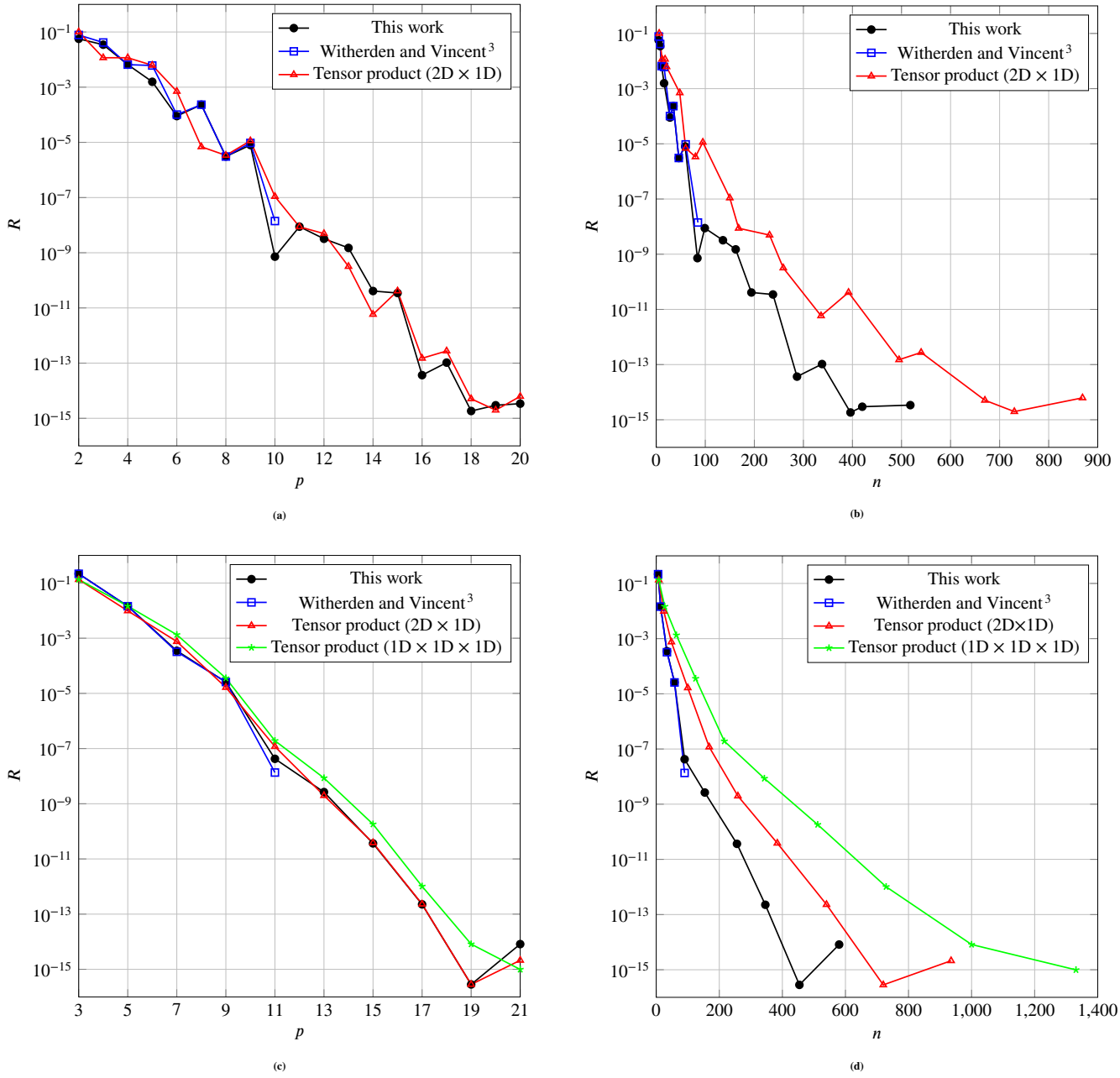

FIGURE 4 Relative error in the integration of the function $\sin(x^2 + y^2)$ over the semi-cylindrical domain using (a), (b) 16 prismatic elements and (c), (d) 8 hexahedral elements with curved faces. Results are shown as a function of p (cubature order) and n (number of cubature nodes).

$p = 10$ and $p = 11$ for the prism and the cube, respectively.[3] As noted in Jaśkowiec and Sukumar[1], the cubature algorithm was very sensitive to the initial guess for the cubature nodes. In this paper, the initial cubature nodes were generated by Cartesian products of lower dimensional cubatures. The polynomial-precision accuracy of the cubature rules were verified and their sound accuracy was affirmed in the integration of nonpolynomial test functions. Numerical tests were also performed using Cartesian product cubature rules over the prism and the hexahedron. For a given p (cubature order), we found that these cubature rules

delivered comparable accuracy to our cubature rules. However, for a given p, our rules required far fewer number of nodes, and for a given n, our rules provided better accuracy—thereby establishing that the cubature rules for the prism and hexahedron proposed herein are more efficient than standard Cartesian product cubature rules over the prism and the hexahedron.

On applying the algorithm in Jaśkowiec and Sukumar,[5] we also constructed non-symmetric cubature rules from $p = 2$ to $p = 20$ over the prism, cube and pyramid (reference elements). These rules have also been verified and their accuracy assessed on the same tests that are reported in this paper. In the supplementary materials, listings of both symmetric and non-symmetric cubature rules (128 digits of precision) are provided.

ACKNOWLEDGEMENTS

The first author gratefully acknowledges the support provided by the Polish-U.S. Fulbright Commission and the Polish National Agency for Academic Exchange via scholarships at the University of California at Davis.

DATA AVAILABILITY STATEMENT

Data available in article supplementary material.

References

1. Jaśkowiec J, Sukumar N. High-order symmetric cubature rules for tetrahedra and pyramids. *International Journal for Numerical Methods in Engineering* 2020. doi: 10.1002/nme.6528

2. Felippa CA. A compendium of FEM integration formulas for symbolic work. *Engineering Computations* 2004; 21(8): 867–890.

3. Witherden FD, Vincent PE. On the identification of symmetric quadrature rules for finite element methods. *Computers & Mathematics with Applications* 2015; 69(10): 1232–1241.

4. Kubatko EJ, Yeager BA, Maggi AL. New computationally efficient quadrature formulas for triangular prism elements. *Computers & Fluids* 2013; 73: 187–201.

5. Jaśkowiec J, Sukumar N. High-order cubature rules for tetrahedra. *International Journal for Numerical Methods in Engineering* 2020; 121(11): 2418–2436.

6. Skala V. Barycentric coordinates computation in homogeneous coordinates. *Computers & Graphics* 2008; 32(1): 120–127.